Full Paper

CONTRAST MEDIA & MOLECULAR IMAGING

Received: 30 March 2011, Revised: 23 June 2011, Accepted: 25 June 2011, Published online in Wiley Online Library: 2011

(wileyonlinelibrary.com) DOI: 10.1002/cmmi.468

Multimodal liposomes for SPECT/MR imaging as a tool for *in situ* relaxivity measurements

Anke de Vries[a†], Maarten B. Kok[a†], Honorius M. H. F. Sanders[a], Klaas Nicolay[a], Gustav J. Strijkers[a] and Holger Grüll[a,b]*

One of the major challenges of MR imaging is the quantification of local concentrations of contrast agents. Cellular uptake strongly influences different parameters such as the water exchange rate and the pool of water protons, and results in alteration of the contrast agent's relaxivity, therefore making it difficult to determine contrast agent concentrations based on the MR signal only. Here, we propose a multimodal radiolabeled paramagnetic liposomal contrast agent that allows simultaneous imaging with SPECT and MRI. As SPECT-based quantification allows determination of the gadolinium concentration, the MRI signal can be deconvoluted to get an understanding of the cellular location of the contrast agent. The cell experiments indicated a reduction of the relaxivity from $2.7 \pm 0.1\ mM^{-1} s^{-1}$ to a net relaxivity of $1.7 \pm 0.3\ mM^{-1} s^{-1}$ upon cellular uptake for RGD targeted liposomes by means of the contrast agent concentration as determined by SPECT. This is not observed for nontargeted liposomes that serve as controls. We show that receptor targeted liposomes in comparison to nontargeted liposomes are taken up into cells faster and into subcellular structures of different sizes. We suggest that the presented multimodal contrast agent provides a functional readout of its response to the biological environment and is furthermore applicable in *in vivo* measurements. As this approach can be extended to several MRI-based contrast mechanisms, we foresee a broader use of multimodal SPECT/MRI nanoparticles to serve as *in vivo* sensors in biological or medical research.

Supporting information may be found in the online version of this paper

Keywords: SPECT; MRI; contrast agent; liposomes; relaxivity; multimodality; quantification; cellular uptake

1. INTRODUCTION

Magnetic resonance imaging (MRI) plays an important role in diagnosis of diseases thanks to its superb soft tissue contrast and high spatial resolution. MR image generation is based on the proton concentration and on the water protons' magnetic properties that are tissue specific. MR contrast between tissues can be further enhanced with contrast agents (CA) that decrease the longitudinal or transversal relaxation times of water protons (T_1 and T_2 respectively). Clinically used T_1 contrast agents commonly are based on gadolinium (Gd) chelates (1), while T_2 agents are based on iron (Fe) oxides (2). For applications in molecular imaging (3), drug delivery (4) or cell tracking (5), accurate means of assessing tissue concentrations of CA are essential. MRI-based quantification of CA concentration can be approached by measurement of the pre- to post-CA-induced changes in the T_1 or T_2 relaxation times. In aqueous media, the relaxivity $r_{1,2}$ ($mM^{-1} s^{-1}$) relates CA concentration (i.e. expressed in terms of Gd or Fe concentration) to the measured relaxation times $T_{1,2}$ (s). *In vivo*, the situation becomes more complex as CA may bind to biological compounds or undergo compartmentalization and internalization, which modulates parameters such as the tumbling and water exchange rates as well as the pool of water protons that can interact with the CA. These effects lead to an agent relaxivity that is different compared with the *in vitro* relaxivity (6–8). In this situation, the apparent disadvantage of MRI can be utilized as a tool to investigate the localization of the CA, provided that the local concentration of CA is known. Any approach to quantitative imaging of contrast agents with MRI and the analysis of the *in vivo* relaxivity of MR agents requires *a priori* a determination of the contrast agent concentration by independent means. Gd concentration measurements in tissue by inductively coupled plasma (ICP) are the gold standard, but can obviously only be applied post-mortem, which restricts this method to fundamental research. Dual modal nanoparticles like fluorine-based emulsions that carry a high payload of Gd-chelates conjugated to the lipid monolayer offer an elegant way to determine the Gd-concentration based on the fluorine signal quantified with MRI (9,10). In principle, this approach is well suited for *in vivo* use in order to probe the effective relaxivity, although it suffers from the low MRI sensitivity for fluorine.

Here we propose a radiolabeled paramagnetic liposome (Fig. 1) as a multimodal agent for SPECT/MRI measurements, where the radiolabel allows quantification of the Gd

* *Correspondence to: H. Grüll, Eindhoven University of Technology, Department of Biomedical Engineering, Biomedical NMR Den Dolech 2 (N-laag 2.62) 5600 MB Eindhoven, the Netherlands.*
E-mail: h.gruell@tue.nl

a *A. de Vries, M. B. Kok, H. M. H. F. Sanders, K. Nicolay, G. J. Strijkers, H. Grüll Biomedical NMR, Department of Biomedical Engineering, Eindhoven University of Technology, Eindhoven, the Netherlands*

b *H. Grüll Department of Bio-molecular Engineering, Philips Research Eindhoven, the Netherlands*

† *The first two authors contributed equally to this paper.*

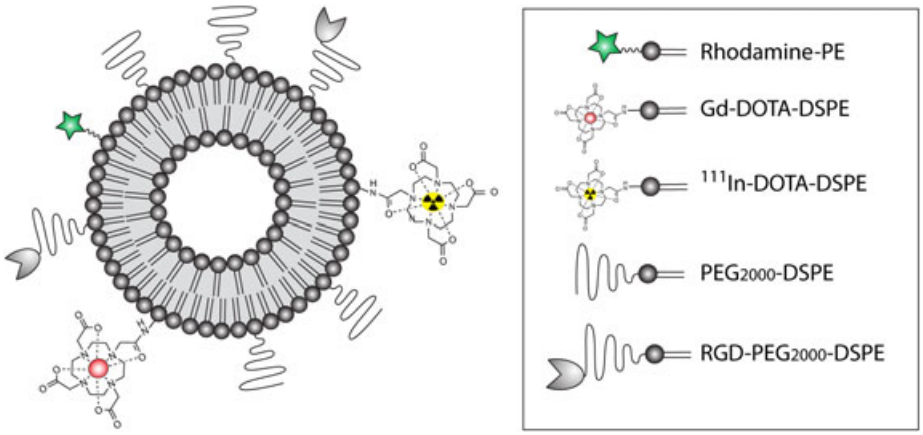

Figure 1. Schematic representation of a multimodal RGD-conjugated liposomal contrast agent. The nanoparticle contains an MR label (Gd-DOTA-DSPE), a radiolabel for SPECT (^{111}In-DOTA-DSPE) and a fluorescent label (Rhodamine-PE).

concentration based on SPECT imaging. This type of multimodal nanoparticle can be employed as a tool to investigate interactions between agent and the biological environment providing the relaxivity as a read-out. We tested this concept *in vitro* with multimodal nanoparticles carrying cyclic RGD peptides to target the $\alpha_v\beta_3$ receptor in comparison to nontargeted liposomes. The $\alpha_v\beta_3$ receptor is typically overexpressed on endothelial cells in angiogenic blood vessels of tumors and is considered a biomarker for cancer (11). Consequently, our *in vitro* study was performed in cell assays using proliferating human umbilical vein derived endothelial cells (HUVECs) as a model system. Earlier cell studies performed with targeted and nontargeted liposomes as well as multimodal fluorine-based emulsions revealed a systematic decrease of the relaxivity for targeted particles upon uptake into HUVECs owing to compartmentalization. Here, liposomes were prepared by thin film hydration and subsequent extrusion following earlier published procedures (12). The liposomal bilayer contained amphiphilic Gd-chelates, a fluorescently labeled lipid based on rhodamine, and an amphiphilic DOTA ligand conjugated to a lipid construct, which later was used for radiolabeling with indium-111 (^{111}In) for SPECT. A maleimide-lipid was furthermore incorporated in the lipid bilayer as a handle to covalently couple cyclic RGD on the liposomal surface for targeting (RGD-liposomes; non-RGD-containing liposomes were used as nontargeted controls and will be further referred to as NT-liposomes). Agent quantification based on SPECT was compared with γ-counting and ICP-MS and used to derive cell-associated relaxivities from relaxation time measurements. Confocal laser scanning microscopy (CLSM) was employed to follow the fate and intracellular localization of the agents.

2. RESULTS AND DISCUSSION

Typically, the final lipid concentration after preparation of the liposomal formulation was approximately 50 mM as determined by phosphate determination according to Rouser *et al.* (13). Size control is of high importance since it may be a critical parameter in the cellular uptake process (14). Dynamic light scattering showed a single peak of 182 and 178 nm for RGD-and NT-liposomes with a polydispersity index of 0.18 and 0.16 respectively. High-resolution cryogenic transmission electron microscopy (cryo-TEM images; figure S1 in Supporting Information) revealed spherical unilamellar vesicles, typical for liposomes, as well as a few micelles, as was observed previously (15). The longitudinal (r_1) and transverse (r_2) relaxivities were determined in a HEPES buffered saline solution at a field strength of 6.3 T and at a temperature of 20 °C, resulting in $r_1 = 2.7 \pm 0.1$ and 3.4 ± 0.1 mM^{-1} s^{-1} and $r_2 = 16.2$ 0.1 and 16.1 ± 0.1 mM^{-1} s^{-1} for RGD-liposomes and NT-liposomes respectively.

To investigate cellular uptake of the multimodal RGD-or NT-liposomes, cultured HUVEC cells were incubated with a liposome-containing medium at a concentration of 1.2 μmol total lipid per ml for 1 up to 8 h. Next, cells were thoroughly washed, collected and centrifuged to obtain loosely packed cell pellets and subsequently imaged with MRI and SPECT/CT. Figure 2 shows MRI, SPECT and overlaid SPECT/CT images of pellets containing HUVECs that were incubated for 8 h with NT-liposomes (Fig. 2A), A), RGD-liposomes (Fig. 2B) and control HUVECs that were not incubated with contrast agent (Fig. 2 C). T_1-weighted MR images show that the pellet containing control HUVECs is essentially iso-intense with the medium above, whereas pellets containing NT-or RGD-incubated HUVECs can easily be distinguished from buffer as a consequence of the reduced T_1. The RGD-incubated cells show higher signal compared with cells incubated with NT-liposomes. Accordingly, SPECT imaging showed a low signal coming from HUVECs incubated with NT-liposomes, and a brighter signal for cells incubated with RGD-liposomes, whereas no activity was found in control HUVECs.

The longitudinal relaxation rates ($R_1 = 1/T_1$) of the cell pellets (Fig. 2D) increased faster after incubation with RGD-liposomes when compared with NT-liposomes, while these differences remained small for the transverse relaxation rate relaxation rates ($R_2 = 1/T_2$; Fig. 2E). However, earlier studies showed that R_1 or R_2 does not allow determination of the intracellular concentration of the paramagnetic nanoparticle (6,7). Compartmentalization into cell organelles may decrease the intracellular relaxivity, which manifests itself in a nonlinear dependence of R_1 on cell-associated contrast agent concentration (8,16). This becomes immediately evident when comparing the MRI data (Fig. 2D) with corresponding SPECT data in Fig. 2(F), which shows the activity per cell pellet after different incubation times with RGD-and NT-liposomes. The cellular uptake of the targeted contrast agent as analyzed with SPECT indicates a faster uptake compared with the apparent uptake kinetics as deduced from the MRI data (Fig. 2D). The SPECT data of Fig. 2(F) indicate a 3.3 times higher uptake of RGD-liposomes compared with NT-liposomes, whereas the R_1 values of Fig. 2(D) show merely a factor of 2.1, pointing to

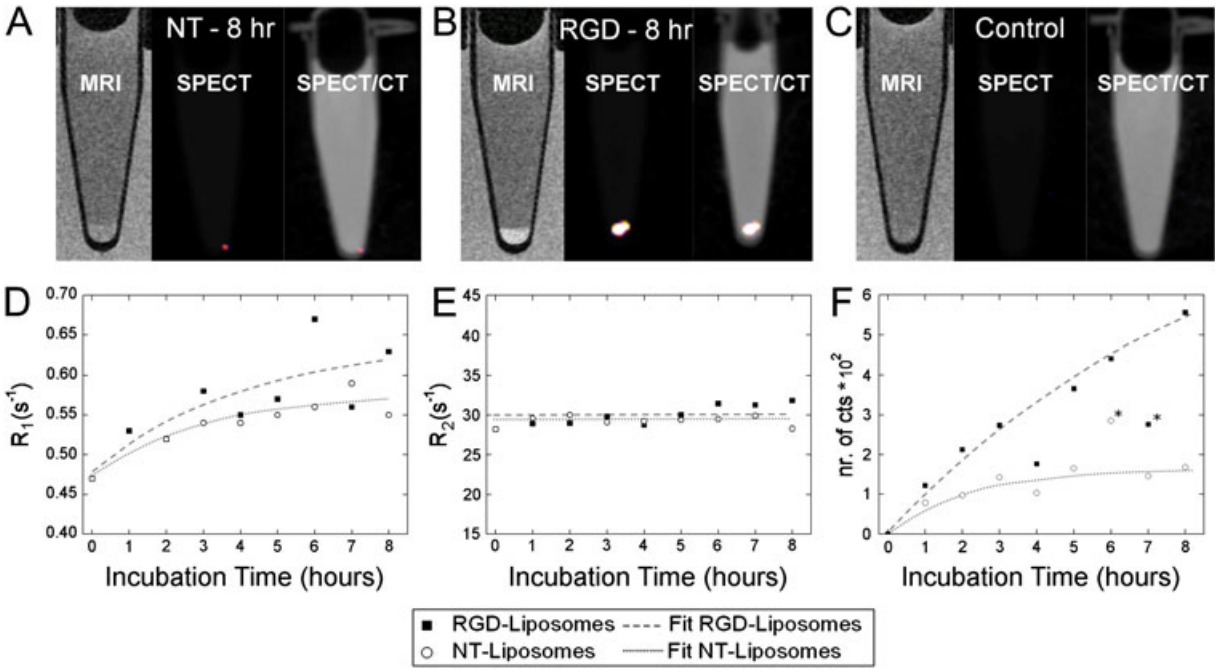

Figure 2. Upper row: T_1-weighted MRI, SPECT and combined SPECT/CT images of pellets of HUVECs incubated for 8 h with NT-liposomes (A), RGD-liposomes (B) and control HUVECs without contrast agent (C). The pellets are situated at the bottom of the Eppendorf cups. Below: uptake of contrast agent as described by R_1-MRI (D) and R_2-MRI (E), and the number of counts (F) in SPECT (background subtracted) as a function of time for HUVECs incubated with RGD-liposomes (solid squares) or NT-liposomes (open circles). All measurements had a typical error of 10–15% (for more details, see Materials and Methods section in the Supporting Information). An exponential fit to the data ($y = y_o + A^*e^{-t/x}$) is provided as a dashed line. Two data points marked with asterisks were not included in the exponential fit.

a systematic decrease of the net relaxivity of targeted liposomes upon cellular uptake. The transverse relaxation rate (Fig. 2E) for both RGD-and NT-liposomes showed similar values throughout the incubation-time range.

For a more detailed analysis, the Gd concentration needed to be related to the activity of ^{111}In. In a dilution series of ^{111}In-labeled liposomes, the ^{111}In signal was measured using scintillation counting of γ-photons, while the Gd concentration was determined with inductively coupled plasma mass spectrometry (ICP-MS). For our multimodal agent, 900 counts from ^{111}In corresponded to 1 nmol Gd, allowing a direct quantification on the amount of Gd within the cells based on the SPECT signal. Beforehand, the SPECT system was calibrated with an ^{111}In source to relate counts to activity (1000 counts corresponded to 2.2 kBq ^{111}In at our reference time). It should be noted that the amount of ^{111}In atoms present in this study was a factor of 10^6 lower than Gd, reflecting the higher sensitivity of SPECT compared with MRI. Nevertheless, the acquired SPECT data (Fig. 2 F) suffer from a low signal-to-noise ratio owing to the overall low activity present in the cell pellets. To verify whether SPECT imaging yields reliable quantitative information in this experiment, the cell pellets were analyzed by ICP and γ-counting for reference. Figure 3 shows the correlation between the Gd content based on SPECT imaging (Fig. 3A) and γ-counting (Fig. 3B) as a function of the Gd content as determined by ICP-MS; a combination of all data finally leads to Fig. 3(C), showing that SPECT imaging indeed allows a reliable quantification of Gd within the cell pellets. In detail, the correlations resulted in $Gd^{3+}_{SPECT} = 0.96 \cdot Gd^{3+}_{ICP\text{-}MS}$ [$R^2 = 0.95$, Pearson's correlation coefficient (r) = 0.93, $p = 0.000$], $Gd^{3+}{}_{\gamma\text{-counting}} = 0.97 \cdot Gd^{3+}_{ICP\text{-}MS}$ ($R^2 = 0.99$, $r = 0.99$, $p = 0.000$) and $Gd^{3+}{}_{SPECT} = 0.87\ Gd^{3+}{}_{\gamma\text{-counting}}$ ($R^2 = 0.95$, $r = 0.93$, $p = 0.000$). Applying this concept *in vivo* would require an application leading to sufficient uptake of the dual modal liposome and to an activity in the lesion that can be reliably quantified with SPECT.

For RGD-liposomes a faster uptake kinetic was observed leading to 0.63 nmol of Gd per cell pellet after 8 h of incubation compared with 0.19 nmol for NT-liposomes. This three-fold difference was previously impossible to detect based on the R_1 signal as shown in Fig. 2(D). The SPECT, ICP-MS and γ-counting calibration (Fig. 3) now allowed analysis of changes of R_1 and R_2 in cells upon incubation with targeted and nontargeted liposomes as a function of the Gd concentration, as measured indirectly with SPECT (Fig. 4A) and volume measurements of the cell pellets by MR. The expected R_1 values as a function of Gd concentration are plotted based on the intrinsic liposomal relaxivity of $r_1 = 2.7$ 0.1 mM^{-1} s^{-1} that was previously determined in HBS buffer (Fig. 4A, solid line). Clearly, all values for R_1 are lower than expected, indicating a reduced intracellular longitudinal relaxivity. The slope taken from the corresponding linear fits allows computation of the apparent intracellular relaxivity for RGD and NT-liposomes (1.73 ± 0.3 vs 2.34 ± 0.7 mM^{-1} s^{-1}), revealing a pronounced reduction of the longitudinal relaxivity for targeted liposomes. The underlying mechanism for the observed effect is the different uptake of targeted and nontargeted liposomes. Internalization by the $\alpha_v\beta_3$ receptor is faster and also leads to a different localization of the targeted nanoparticle compared with nontargeted liposomes (7). No significant R_2 differences were observed between RGD-and NT-liposomes treated cells at any time point.

The cellular location of the liposomal contrast agent was determined using confocal laser scanning microscopy (CLSM), by using the rhodamine fluorphor present in the bilayer of the liposomes. Figure 5 shows confocal images of HUVECs grown on gelatin-coated coverslips. Both RGD-and NT-liposomes accumulated in the perinuclear region. Until 8 h of incubation, both the

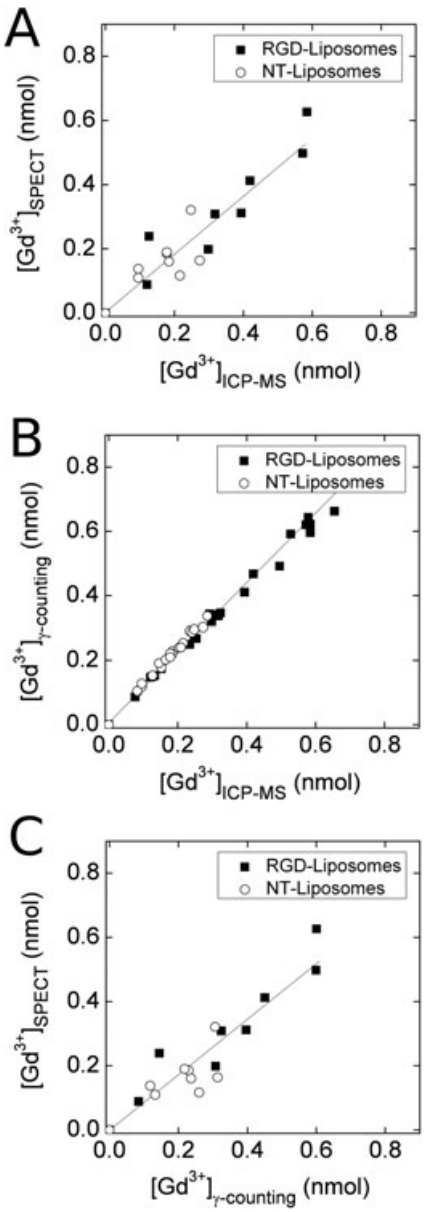

Figure 3. Gadolinium content calculated from SPECT (A), γ-counting (B) as a function of the amount of gadolinium determined by ICP-MS; amount of gadolinium calculated from SPECT correlated to gadolinium content as calculated from γ-counting data (C) for HUVECs incubated with RGD-liposomes (solid squares) or NT-liposomes (open circles). The solid line is a linear fit to all experimental data resulting in $Gd^{3+}_{SPECT} = 0.96 \cdot Gd^{3+}_{ICP\text{-}MS}$ [$R^2 = 0.95$, Pearson's correlation coefficient (r) = 0.93, $p = 0.000$], $Gd^{3+}_{\gamma\text{-counting}} = 0.97 \cdot Gd^{3+}_{ICP\text{-}MS}$ ($R^2 = 0.99$, $r = 0.99$, $p = 0.000$) and $Gd^{3+}_{SPECT} = 0.87 \cdot Gd^{3+}_{\gamma\text{-counting}}$ ($R^2 = 0.95$, $r = 0.93$, $p = 0.000$).

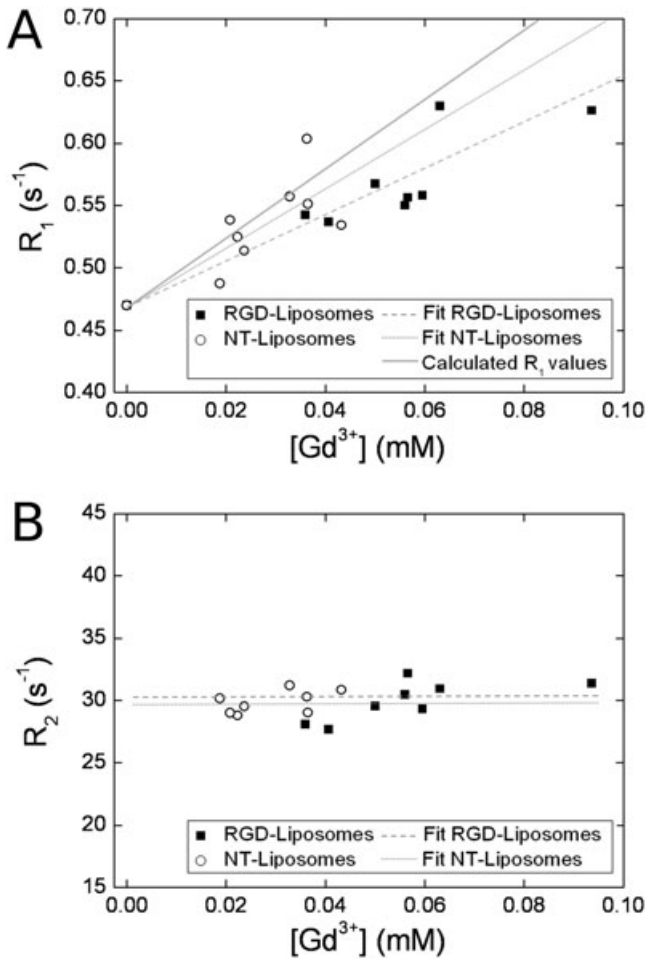

Figure 4. ^{1}H relaxometry measurements for pellets of HUVECs incubated with RGD-liposomes (solid squares) or NT-liposomes (open circles). R_1 (A) and R_2 (B) as a function of the concentration of gadolinium as determined by SPECT. Data fits are provided as a dashed (RGD-liposomes) and dotted (NT-liposomes) line. The solid line in (A) represents the calculated R_1 values that should have been observed if the relaxivity was not quenched and was found to be significantly different from the RGD-liposomes in HUVECs ($p < 0.05$).

RGD-and NT-liposomes were mainly found in sharply delineated spherical structures 0.4–1.0 μm diameter inside the cytoplasm. No detectable association of liposomes with the cellular membrane was observed for both RGD-and NT-liposomes. Clear differences in uptake between RGD-and NT-liposomes were visible. For HUVECs incubated with RGD-liposomes, many significantly larger vesicular structures with a diameter of 1–5 μm were observed, indicating concentrated spots of RGD-liposomes. On the other hand, incubation with NT-liposomes resulted in a perinuclear intracellular distribution in smaller 0.4–1.0 μm diameter vesicles. A three-compartment exchange model as previously published by Strijkers *et al.* (8) showed that the lower surface-to-volume ratio for larger sized vesicles compared with small vesicles results in a reduced water exchange across the vesicular membrane, which again translates into a reduced longitudinal relaxivity. This observed reduction can be ascribed to the endocytotic uptake of RGD targeted liposomes into larger vesicles (Fig. 4A).

3. CONCLUSIONS

Previously, liposomes have been investigated as a combined SPECT and MRI contrast agent (17–21); however, these studies did not address quantification to aid in the interpretation of MRI parameter changes. In our study, we demonstrated that dual modal nanoparticles can be utilized in SPECT to measure the particle concentration. The presented dual-modality approach can give a better understanding of the cellular location of the contrast agent as its concentration can be determined by SPECT while MRI is used to measure the relaxivity. As the latter is

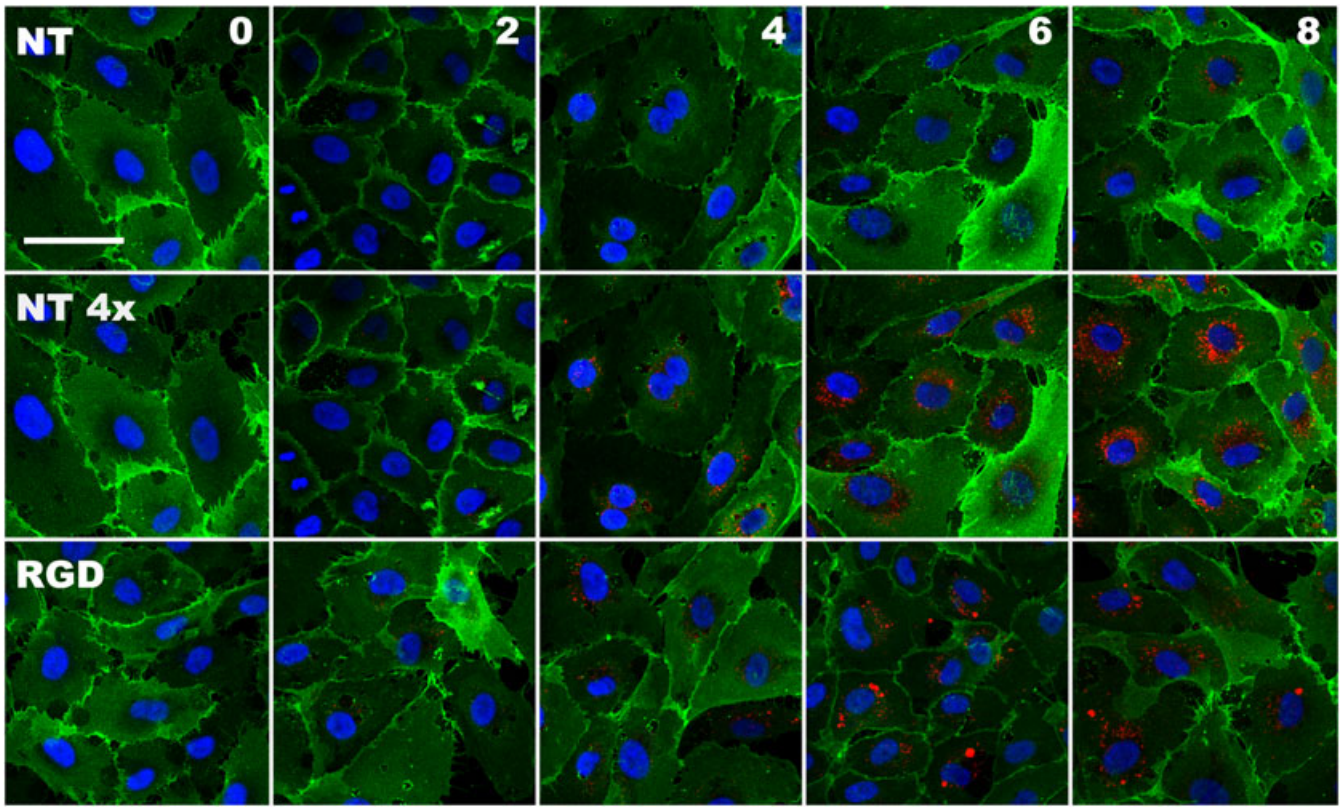

Figure 5. CLSM images of HUVECs incubated with RGD-liposomes (RGD) or NT-liposomes (NT). Blue, DAPI; red, rhodamine; green, CD31; bar, 50 μm. The number shown in the top right corner of each column refers to the incubation time in hours. Note that the laser intensity used to obtain NT 4× images (middle row) was four-fold higher than the intensity used to obtain the other images (bottom and top row).

modulated by the intracellular location (i.e. endosome, cytosol), the net relaxivity provides indirect information about the fate of the contrast agent upon cellular uptake. This approach may be easily extended to multimodal SPECT/MRI and also PET/MRI nanoparticles to measure other functional MR-based signals, as was previously demonstrated for pH-mapping (22,23). Other examples range from smart MR probes to report temperature and enzyme activity based on different concepts such as CEST agents (24,25), enzyme-responsive paramagnetic liposomal contrast agents (26) to MR image-guided drug delivery systems (4,27) and cellular trafficking (5), where the alterations in the MRI signal are a convolution of MR contrast agent concentration and a response to the environment. As this approach is noninvasive and applicable *in vivo* in longitudinal studies, a broad utility of this concept can be expected in imaging-based analyses in biological and medical research.

4. EXPERIMENTAL

4.1. Materials

1,2-Distearoyl-*sn*-glycero-3-phosphocholine (DSPC), cholesterol, 1,2-distearoyl-*sn*-glycero-3-phosphoethanolamine-*N*-[methoxy (polyethyleneglycol)-2000] (PEG_{2000}-DSPE), 1,2-distearoyl-*sn*-glycero-3-phosphoethanolamine-*N*-[maleimide(polyethyleneglycol)-2000] (Mal-PEG_{2000}-DSPE) and 1,2-dipalmitoyl-*sn*-3-phosphoethanolamine-*N*-[lissamine rhodamine B sulfonyl) (rhodamine-PE) were obtained from Avanti Polar Lipids (Alabaster, AL, USA). 1,2-Distearoyl-*sn*-glycero-3-phosphpethanolamine-[tetraazacyclododecane tetraacetic acid] (Gd-DOTA-DSPE) and DOTA-DSPE were purchased from SyMO-Chem (Eindhoven, the Netherlands). Endothelial Growth Medium-2 (EGM-2) and HUVECs were ordered with Lonza Bioscience (Switzerland). Monoclonal mouse anti-human CD31 antibody was obtained from Dakocytomation (Glostrup, Denmark). Alexa Fluor 488 conjugated goat anti-mouse secondary antibody was obtained from Molecular Probes Europe BV (Leiden, the Netherlands). Cyclic RGD, c[RGDf(−S-acetylthioacetyl)K] was synthesized by Ansynth Service BV (Roosendaal, the Netherlands). ^{111}In originated from Perkin Elmer (Boston, MA, USA). All other chemicals were obtained from Sigma (St Louis, MO, USA) and were of analytical grade or the best grade available.

4.2. Liposome preparation and characterization

The 200 nm-diameter liposomes containing Gd-DOTA-DSPE, DOTA-DSPE, DSPC, cholesterol, PEG_{2000}-DSPE and Mal-PEG_{2000}-DSPE at a molar ratio of 0.72:0.03:1.10:1:0.075:0.075 were produced by lipid film hydration and extrusion (400 μmol lipids in total). Briefly, the lipids were dissolved in a 1:5 *v/v* methanol–chloroform mixture. As a fluorescent marker, 0.1 mol% of rhodamine-PE was added. A lipid film was created by drying *in vacuo*. The lipid film was hydrated at 67 °C using a HEPES buffered saline solution (HBS), containing 20 mM HEPES and 135 mM NaCl (pH 6.7). The lipid suspension was extruded at 67 °C, twice through a single 200 nm polycarbonate membrane (Whatman,

Kent, UK) and six times through a double 200 nm polycarbonate membrane. After extrusion, half of the liposome suspension was modified with a cyclic RGD-peptide (6 μg μmol^{-1} total lipid) to target the $\alpha_v\beta_3$-integrin. The cyclic RGD-peptide was deacetylated and coupled to the distal end of Mal-PEG$_{2000}$-DSPE. After incubation overnight at 4 °C, both batches of liposomes were centrifuged at 310 000 *g* for 45 min in order to remove possible unconjugated RGD-peptide for the batch containing RGD-liposomes. The pellets were resuspended in HBS (pH 7.4). Lipid concentration was measured by phosphate determination according to Rouser *et al*. (13). Size and polydispersity index of the liposomes were determined with dynamic light scattering (Zetasizer Nano, Malvern, UK). Cryogenic transmission electron microscopy pictures were obtained with a FEI TECNAI F30ST electron microscope operated at an accelerating voltage of 300 kV. Sample preparation was performed by applying a 4 μl droplet of suspension to a holey carbon film and subsequently plunge-freezing this sample into liquid ethane using a Vitrobot. Both the longitudinal and transverse relaxivity were determined at 6.3 T (20 °C) by fitting R_1 ($1/T_1$) and R_2 ($1/T_2$) values as a function of the Gd concentration of the liposome suspension as determined using inductively coupled plasma atomic mass spectroscopy (ICP-MS) by Philips Research (Eindhoven, the Netherlands), using the least squares method.

4.3. ^{111}Indium labeling

RGD-liposomes and NT-liposomes were labeled with ^{111}indium (Perkin Elmer, Boston, MA, USA). In detail, 100 μl ammonium acetate buffer (2 M NH_4OAc, pH 4.5) was added to a 2.6 ml liposomal solution together with 25 μl of ^{111}Indium (50 MBq) and the pH was adjusted to 5.0. The sample was stirred at 50 °C for 90 min. Free DTPA (10 μl, 10 mM) was added to the reaction mixture for 15 min to scavenge free radionuclides. Labeling efficiency was checked on silica TLC using 200 mM EDTA as mobile phase and analyzed using a Phosphor Imager (FLA-7000, Fujifilm, Tokyo, Japan). Radiochemical purities obtained were >95% for the RGD-liposomes as well as the NT-liposomes.

4.4. Cell culture

Human umbilical vein-derived endothelial cells were used for all the experiments. Cells were stored in liquid nitrogen upon arrival. Before use, the cells were quickly thawed in a water bath (37 °C) and divided between two gelatin-coated T75 TCPS flasks (VWR, West Chester, PA, USA). Cells were cultured in a humidified incubator at 37 °C with 5% CO_2. The EGM-2 medium was replaced every 2–3 days. Cells were subcultured at 80–90% confluency according to procedures provided by Lonza Bioscience (Switzerland).

4.5. Experimental setup

Cells of passage 3 or 4 were used for all experiments at 80–90% confluency. Incubation was carried out on both gelatin-coated coverslips, for CLSM analysis, and in gelatin-coated T75 TCPS culture flasks, for MRI, FACS and ICP-MS analysis. Samples for CLSM were incubated with liposomes that were not labeled with ^{111}Indium. All measurements were done in triplicate for both types of liposomes and each incubation time. To start the experiment, medium was replaced by either RGD-liposome or NT-liposome containing medium at a concentration of 1.2 μmol total lipid ml^{-1}. A 4 ml aliquot of liposome containing medium was added to the T75 gelatin-coated TCPS flasks and 0.5 ml of medium was added to the gelatin-coated coverslips. The incubation time with liposomes containing medium was varied between 0 and 8 h. After incubation, the cells were washed three times with 5 ml pre-warmed (37 °C) HEPES-buffered saline solution to remove nonadherent liposomes. After these washing steps, the cells grown on coverslips were fixed using 4% PFA for 15 min at room temperature. Cells in culture flasks were detached using 2 ml 0.25% trypsin 1 mM EDTA·4Na (Lonza Bioscience, Switzerland). The trypsin solution was neutralized using 4 ml trypsin neutralizing solution (Lonza Bioscience, Basel, Switzerland). Cells were spun down at 220 ***g*** and the supernatant was removed. The cell pellet was resuspended in 200 μl 4% paraformaldehyde solution in phosphate-buffered saline (PBS) and transferred to a 300 μl Eppendorf cup. A loosely-packed cell pellet was formed by centrifugation at 10 ***g*** for 5 min. The 51 cell pellets (three control, 24 NT-liposome containing and 24 RGD-liposome containing cell pellets) were stored at room temperature in the dark.

4.6. Magnetic resonance imaging

The T_1 and T_2 relaxation times and the volume of the 51 pellets were measured using a 6.3 T horizontal bore animal MR scanner (Bruker, Ettlingen, Germany). Samples were measured approximately 3 months after initial labeling. After this period the radioactivity was reduced to safe levels for handling. All measurements were carried out at room temperature. Longitudinal and transverse relaxation times were measured in a 3 cm diameter send-and-receive quadrature-driven birdcage coil (Rapid Biomedical, Rimpar, Germany). The Eppendorf tubes containing the loosely packed cell pellets were placed in a custom made holder (four tubes at a time) that was filled with HEPES buffered saline solution to facilitate shimming. T_1 was measured using a fast inversion recovery segmented FLASH sequence with an echo time (*TE*) of 1.5 ms, a repetition time (*TR*) of 3.0 ms, a flip angle of 15º, and an inversion time (*TI*) ranging from 67 to 4800 ms in 80 steps. Overall repetition time was 20 s. Field of view (FOV) was 3×2.18 cm^2, using a matrix size of 128x128, a slice thickness of 0.75 mm and 2 averages. T_2 was measured using a multislice multiecho sequence with *TE* ranging between 9 and 288 ms in 32 steps and a *TR* of 1000 ms. The FOV was 3×2.2 cm^2 and slice thickness was 0.75 mm using a matrix size of 128×128. The number of averages was 4. From the images T_1-and T_2-maps were calculated using Mathematica (Wolfram Research Inc, Champaign, IL, USA). The T_1 and T_2 of the different cell pellets were determined by selecting a ROI within the pellet. T_1-weighted images were measured using a multislice spin-echo sequence with $TE = 10.3$ ms and $TR = 500$ ms. The FOV was 3×2.18 cm^2 and slice thickness was 0.75 mm using a matrix size of 256×192. The number of averages was 1. The volume of the cell pellet was determined for each sample separately in a 0.7 cm diameter solenoid coil using a 3D FLASH sequence with $TE = 3.2$ ms, $TR = 25$ ms and a flip angle of 30º. The FOV was 1.6×1.6 1.6 cm^3, and matrix size was $128 \times 128 \times 128$. Number of averages was 1. A threshold value was determined manually to select the voxels inside the pellet, which were multiplied by the voxel volume to obtain the total volume of the pellet. The concentration of Gd in each cell pellet was determined by dividing the gadolinium content by the pellet volume.

4.7. SPECT imaging and quantification

Measurements were performed on 17 cell pellets (one control, eight NT-liposome containing-and eight RGD-liposome containing cell pellets) using the Bioscan nanoSPECT/CT system (Washington, DC, USA). Owing to the radioactive decay of ^{111}Indium, we were limited to measuring only some of the 51 cell pellets. For the helical SPECT scan 48 projections were obtained with 960 s per projection using 20% windows centered at 171 keV and a 15% window centered at 245 keV. Subsequently, a helical CT scan was made for overlay using 45 keV, 177 μA, 2000 ms, 360 projections and a pitch of 1. After reconstruction voxel sizes were obtained of 1.2 mm^3 (SPECT) and 0.5 mm^3 (CT). Cellular uptake of ^{111}indium was determined by drawing at least three different volumetric regions of interest (ROIs) around the cell pellets using InVivoScope software (Bioscan). The background was determined using exact copies of the ROIs drawn around the cell pellets (at least three per vial), but now in an area without any measurable radioactivity. Quantitative cellular uptake was obtained after a subtraction of the obtained SPECT signal within the cell pellets with the background signal. Calculated errors were typically 10–15% of the total signal and were derived from the signal error of the ROIs within the vial and the background error. All 51 cell pellets were furthermore measured using a γ-counting wizard (Wizard 1480 3" Wallac counter, Perkin Elmer, Groningen, the Netherlands) as a control measurement for quantitative analysis. Also here a background correction was performed.

4.8. Statistical analysis

For the correlation of the different quantification techniques, Pearson's correlation coefficient (r) was computed. ANOVA tables were used to calculate the p-values of the three correlation plots, determining whether there is a statistically significant relationship between SPECT vs ICP-MS, γ-counting vs ICP-MS and SPECT vs γ-counting quantification at the 95% confidence interval. No outliers were removed. The relaxivity values of the RGD-liposomes in cells (Fig. 4A) were compared with the calculated r_1 using a two-sided Student's t-test with a 95% confidence interval.

4.9. Determination of the phosphorus and gadolinium concentration by ICP-MS

Phosphorus and Gd concentrations of the liposome mixtures as well as those from the obtained cell pellets were determined by means of inductively coupled plasma-mass spectrometry (ICP-MS, DRCII, Perkin Elmer) after the destruction with nitric acid at 180 °C.

4.10. Confocal laser scanning microscopy

After fixation, the coverslips with HUVECs incubated with liposomes were stained using a mouse anti-human CD31 antibody to visualize the cellular membrane. The cells were rinsed for 5 min with PBS followed by 60 min of incubation with the primary mouse anti-human CD31 antibody (1:40 dilution). Subsequently the cells were washed for 3 × 5 min with PBS followed by 30 min of incubation with a secondary Alexa Fluor 488 goat anti-mouse IgG antibody (1:200 dilution). The cells were washed for 3 × 5 min with PBS and the nuclei were stained for 5 min with DAPI. After staining of the nuclei the cells were rinsed for 3 × 5 min with PBS and subsequently mounted on a microscopy slide using Mowiol mounting medium. Confocal fluorescence images were recorded at room temperature on a Zeiss LSM 510 META system using a Plan-Apochromat® 63×/1.4 NA oil-immersion objective. Alexa Fluor 488 and rhodamine-PE were excited using the 488 and 543 nm line of a HeNe laser, respectively. The fluorescence emission of Alexa Fluor 488 was recorded with photomultiplier tubes (Hamamatsu R6357) after spectral filtering with a NFT 490 nm beam splitter followed by a 500–550 nm bandpass filter. Rhodamine-PE emission was analyzed using the Zeiss Meta System in a wavelength range of 586–704 nm. DAPI staining of nuclei was visualized by two-photon excitation fluorescence microscopy performed on the same Zeiss LSM 510 system. Excitation at 780 nm was provided by a pulsed Ti–sapphire laser (Chameleon™; Coherent, Santa Clara, CA, USA), and fluorescence emission was detected with a 395–465 nm bandpass filter. All experiments were combined in multitrack mode and acquired confocally.

Acknowledgments

This study was funded in part by the BSIK program entitled Molecular Imaging of Ischemic Heart Disease (project number BSIK03033), the Integrated EU Project MEDITRANS (FP6-2004-NMP-NI-4/IP 026668–2) and the EC-FP6-project DiMI, LSHB-CT-2005-512146. This study was performed in the framework of the European Cooperation in the field of Scientific and Technical Research (COST) D38 Action Metal-Based Systems for Molecular Imaging Applications. The authors would like to express their thanks to Jeannette Smulders for the ICP-MS analysis and Sander Langereis for helpful discussions.

REFERENCES

1. Caravan P, Ellison JJ, McMurry TJ, Lauffer RB. Gadolinium(III) chelates as MRI contrast agents: structure, dynamics, and applications. Chem Rev 1999; 99(9): 2293–2352.
2. Laurent S, Forge D, Port M, Roch A, Robic C, Vander Elst L, Muller RN. Magnetic iron oxide nanoparticles: synthesis, stabilization, vectorization, physicochemical characterizations, and biological applications. Chem Rev 2008; 108(6): 2064–2110.
3. Terreno E, Castelli DD, Viale A, Aime S. Challenges for molecular magnetic resonance imaging. Chem Rev 2010; 110(5): 3019–3042.
4. Hynynen K. MRI-guided focused ultrasound treatments. Ultrasonics 2010; 50(2): 221–229.
5. Bulte JW. In vivo MRI cell tracking: clinical studies. AJR Am J Roentgenol 2009; 193(2): 314–325.
6. Geninatti Crich S, Cabella C, Barge A, Belfiore S, Ghirelli C, Lattuada L, Lanzardo S, Mortillaro A, Tei L, Visigalli M, Forni G, Aime S. In vitro and in vivo magnetic resonance detection of tumor cells by targeting glutamine transporters with Gd-based probes. J Med Chem 2006; 49(16): 4926–4936.
7. Kok MB, Hak S, Mulder WJ, van der Schaft DW, Strijkers GJ, Nicolay K. Cellular compartmentalization of internalized paramagnetic liposomes strongly influences both T_1 and T_2 relaxivity. Magn Reson Med 2009; 61(5): 1022–1032.
8. Strijkers GJ, Hak S, Kok MB, Springer CS, Jr., Nicolay K. Three-compartment T_1 relaxation model for intracellular paramagnetic contrast agents. Magn Reson Med 2009; 61(5): 1049–1058.
9. Kok MB, de Vries A, Abdurrachim D, Prompers JJ, Grull H, Nicolay K, Strijkers GJ. Quantitative (1)H MRI, (19)F MRI, and (19)F MRS of cell-internalized perfluorocarbon paramagnetic nanoparticles. Contrast Media Mol Imaging 2010; 6(1): 19–27.
10. Morawski AM, Winter PM, Yu X, Fuhrhop RW, Scott MJ, Hockett F, Robertson JD, Gaffney PJ, Lanza GM, Wickline SA. Quantitative 'magnetic resonance immunohistochemistry' with ligand-targeted (19)F nanoparticles. Magn Reson Med 2004; 52(6): 1255–1262.
11. Brooks PC, Clark RA, Cheresh DA. Requirement of vascular integrin alpha v beta 3 for angiogenesis. Science 1994; 264(5158): 569–571.

12. Mulder WJM, Strijkers GJ, Griffioen AW, van Bloois L, Molema G, Storm G, Koning GA, Nicolay K. A Liposomal system for contrast-enhanced magnetic resonance imaging of molecular targets. Bioconjug Chem 2004; 15(4): 799–806.
13. Rouser G, Fkeischer S, Yamamoto A. Two dimensional then layer chromatographic separation of polar lipids and determination of phospholipids by phosphorus analysis of spots. Lipids 1970; 5(5): 494–496.
14. Allen TM, Austin GA, Chonn A, Lin L, Lee KC. Uptake of liposomes by cultured mouse bone marrow macrophages: influence of liposome composition and size. Biochim Biophys Acta 1991; 1061(1): 56–64.
15. Hak S, Sanders HM, Agrawal P, Langereis S, Grull H, Keizer HM, Arena F, Terreno E, Strijkers GJ, Nicolay K. A high relaxivity Gd(III)DOTA-DSPE-based liposomal contrast agent for magnetic resonance imaging. Eur J Pharm Biopharm 2009; 72(2): 397–404.
16. Delli Castelli D, Dastru W, Terreno E, Cittadino E, Mainini F, Torres E, Spadaro M, Aime S. In vivo MRI multicontrast kinetic analysis of the uptake and intracellular trafficking of paramagnetically labeled liposomes. J Control Release 2010; 144(3): 271–279.
17. Li D, Patel AR, Klibanov AL, Kramer CM, Ruiz M, Kang BY, Mehta JL, Beller GA, Glover DK, Meyer CH. Molecular imaging of atherosclerotic plaques targeted to oxidized LDL receptor LOX-1 by SPECT/CT and magnetic resonance. Circul Cardiovasc Imaging 2010; 3(4): 464–472.
18. Lijowski M, Caruthers S, Hu G, Zhang H, Scott MJ, Williams T, Erpelding T, Schmieder AH, Kiefer G, Gulyas G, Athey PS, Gaffney PJ, Wickline SA, Lanza GM. High sensitivity: high-resolution SPECT-CT/MR molecular imaging of angiogenesis in the Vx2 model. Invest Radiol 2009; 44(1): 15–22.
19. Torchilin VP. Surface-modified liposomes in gamma- and MR-imaging. Adv Drug Deliv Rev 1997; 24: 301–313.
20. Zielhuis SW, Seppenwoolde JH, Mateus VA, Bakker CJ, Krijger GC, Storm G, Zonnenberg BA, van het Schip AD, Koning GA, Nijsen JF. Lanthanide-loaded liposomes for multimodality imaging and therapy. Cancer Biother Radiopharm 2006; 21(5): 520–527.
21. Hu G, Lijowski M, Zhang H, Partlow KC, Caruthers SD, Kiefer G, Gulyas G, Athey P, Scott MJ, Wickline SA, Lanza GM. Imaging of Vx-2 rabbit tumors with alpha(nu)beta3-integrin-targeted ^{111}In nanoparticles. Int J Cancer 2007; 120(9): 1951–1957.
22. Frullano L, Catana C, Benner T, Sherry AD, Caravan P. Bimodal MR-PET agent for quantitative pH imaging. Angew Chem Int Edn Engl 2010; 49(13): 2382–2384.
23. Gianolio E, Maciocco L, Imperio D, Giovenzana GB, Simonelli F, Abbas K, Bisi G, Aime S. Dual MRI-SPECT agent for pH-mapping. Chem Commun (Camb) 2011; 47(5): 1539–1541.
24. Terreno E, Castelli DD, Aime S. Encoding the frequency dependence in MRI contrast media: the emerging class of CEST agents. Contrast Media Mol Imag 2010; 5(2): 78–98.
25. Yoo B, Raam MS, Rosenblum RM, Pagel MD. Enzyme-responsive PARACEST MRI contrast agents: a new biomedical imaging approach for studies of the proteasome. Contrast Media Mol Imag 2007; 2(4): 189–198.
26. Figueiredo S, Moreira JN, Geraldes CF, Aime S, Terreno E. Supramolecular protamine/Gd-loaded liposomes adducts as relaxometric protease responsive probes. Bioorg Med Chem 2011; 19(3): 1131–1135.
27. de Smet M, Heijman E, Langereis S, Hijnen NM, Grüll H. Magnetic resonance imaging of high intensity focused ultrasound mediated drug delivery from temperature-sensitive liposomes: An in vivo proof-of-concept study. J Control Release 2011; 150(1): 102–110.